

NLO QCD CORRECTIONS TO INCLUSIVE J/ψ AND Υ PHOTOPRODUCTION CROSS SECTIONS AT THE EIC

Yelyzaveta Yedelkina

July 24, 2022

EIC User Group Early Career Workshop 2022, CFNS Stony Brook University
24-25 July 2022



This project is supported by the European Union's Horizon 2020 research and innovation programme under Grant agreement no. 824093, the French Agence Nationale de la Recherche (ANR) via the grant ANR-20-CE31-0015 ("PrecisOnium") and by the "ADI 2021" project funded by the IDEX

Introduction: inclusive $J/\psi(\Upsilon)$ photoproduction

C.-H. Chang, NPB172, 425 (1980); R. Baier & R. Rückl Z. Phys. C 19, 251(1983);

We will discuss **inclusive $J/\psi(\Upsilon)$ photoproduction**:

- $J/\psi(\Upsilon)$ is a $c\bar{c}$ ($b\bar{b}$) bound state with $J = 1$, $L = 0$, $S = 1$; **vector** particle
- **inclusive photoproduction**:

$$\gamma(Q^2 \simeq 0) + p \rightarrow J/\psi + X;$$

- We will discuss the photoproduction at **NLO**;

Introduction: inclusive $J/\psi(\Upsilon)$ photoproduction

C.-H. Chang, NPB172, 425 (1980); R. Baier & R. Rückl Z. Phys. C 19, 251(1983);

We will discuss **inclusive $J/\psi(\Upsilon)$ photoproduction**:

- $J/\psi(\Upsilon)$ is a $c\bar{c}$ ($b\bar{b}$) bound state with $J = 1$, $L = 0$, $S = 1$; **vector** particle
- **inclusive photoproduction**:

$$\gamma(Q^2 \simeq 0) + p \rightarrow J/\psi + X;$$

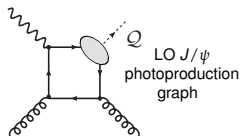
- We will discuss the photoproduction at **NLO**;
- **3 common models** (differences in the treatment of the hadronisation):
 - ▶ **Colour Singlet Model**;
 - ▶ NRQCD and Colour Octet Mechanism;
 - ▶ Colour Evaporation Model;

Basic pQCD approach: the Colour Singlet Model (CSM)

C.-H. Chang, NPB172, 425 (1980); R. Baier & R. Rückl Z. Phys. C 19, 251(1983);

One supposes two **factorisations**:

- 1 **collinear**, in which the hadronic cross section can be written as the convolution of the **PDFs** with the **partonic cross section**;
- 2 between the hard part (a perturbative amplitude, which describes the $Q\bar{Q}$ **pair production**) and the soft part (a non-perturbative matrix element, which describes **hadronisation**):
 - Perturbative creation of 2 quarks, Q and \bar{Q}
 - ▶ on-shell
 - ▶ in a colour singlet state
 - ▶ with a vanishing relative momentum
 - ▶ in a 3S_1 state (for J/ψ , ψ' and Υ)
 - Non-perturbative binding of quarks
→ Schrödinger wave function at $r = 0$

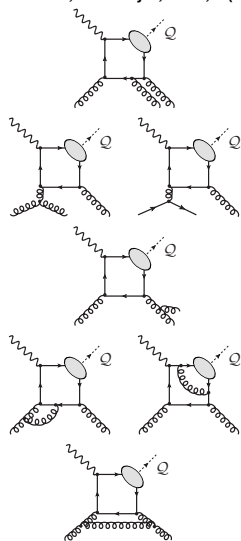


CSM: the Taylor series expansion of the amplitude in the $Q\bar{Q}$ relative momentum (v) to the first non-vanishing (Leading- v NRQCD) term.

General structure of NLO corrections

M. Krämer, Nucl.Phys., B459, 3 (96')

Singularities at NLO [and how they are removed]:



- Real emission

- ▶ Infrared divergences: Soft [cancelled by loop IR contr.]
- ▶ Infrared divergences: Collinear
 - ★ initial state [subtracted via “renormalisation” of collinear PDFs (Altarelli-Parisi counter-terms)]
 - ★ final state [cancelled by loop IR contr.]

- Virtual (loop) contribution

- ▶ Ultraviolet divergences: [removed by renormalisation]
- ▶ Infrared divergences: [cancelled by real Infrared contribution]

- We use the **FDC** code [J.-X. Wang Nucl.Instrum.Meth. A534(2004)241-245] to produce NLO results

[The quark and antiquark attached to the blob are taken as on-shell and their relative velocity v is set to zero.]

Part I

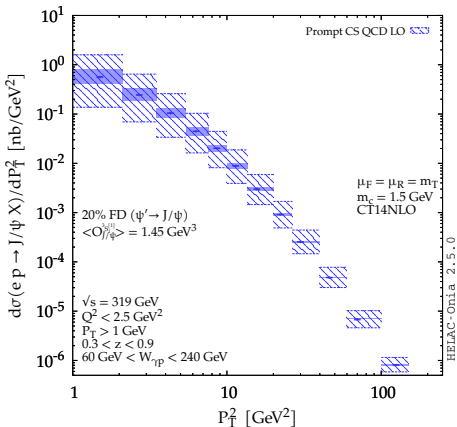
Photoproduction at mid and high P_T at HERA

Different contributions in the CSM up to NLO

NLO*: C.Flore, J.-P. Lansberg, H.S. Shao, Y. Yedelkina, PLB 811 (2020) 135926

Different contributions in the CSM up to NLO

NLO*: C.Flore, J.-P. Lansberg, H.S. Shao, Y. Yedelkina, PLB 811 (2020) 135926



$$\gamma + g \rightarrow \psi + g @ \alpha\alpha_s^2$$

Notes:

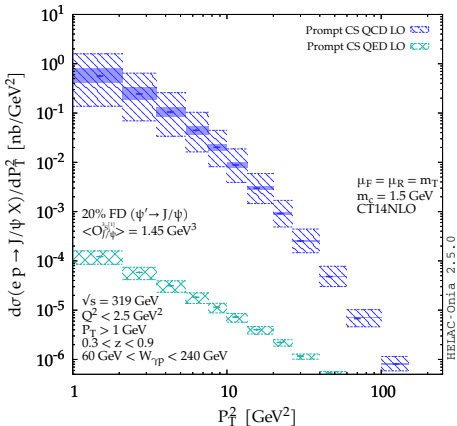
The computations were done with HELAC-ONIA and FDC. The scale and mass uncertainties are shown by the hatched and solid bands.

HELAC-Onia: **H.S. Shao, CPC198 (2016) 238**; FDC: **J.-X. Wang Nucl.Instrum.Meth.**

A534(2004)241-245; See also <https://nloaccess.in2p3.fr>

Different contributions in the CSM up to NLO

NLO*: C.Flore, J.-P. Lansberg, H.S. Shao, Y. Yedelkina, PLB 811 (2020) 135926



$$\gamma + g \rightarrow \psi + g @ \alpha\alpha_s^2$$



$$\gamma + q \rightarrow \psi + q @ \alpha^3 \text{ [NEW !]}$$

Notes:

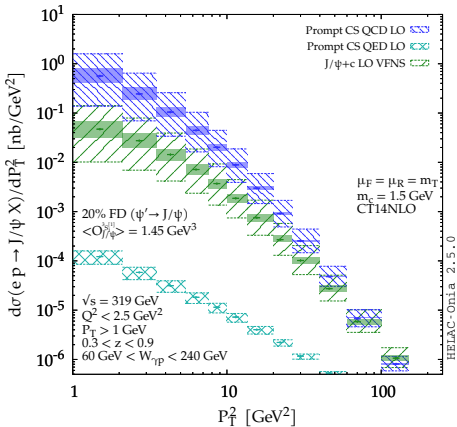
The computations were done with HELAC-ONIA and FDC. The scale and mass uncertainties are shown by the hatched and solid bands.

HELAC-Onia: H.S. Shao, CPC198 (2016) 238; FDC: J.-X. Wang Nucl.Instrum.Meth.

A534(2004)241-245; See also <https://nloaccess.in2p3.fr>

Different contributions in the CSM up to NLO

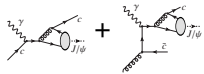
NLO*: C.Flore, J.-P. Lansberg, H.S. Shao, Y. Yedelkina, PLB 811 (2020) 135926



$$\gamma + g \rightarrow \psi + g @ \alpha \alpha_s^2$$



$$\gamma + q \rightarrow \psi + q @ \alpha^3 \text{ [NEW !]}$$

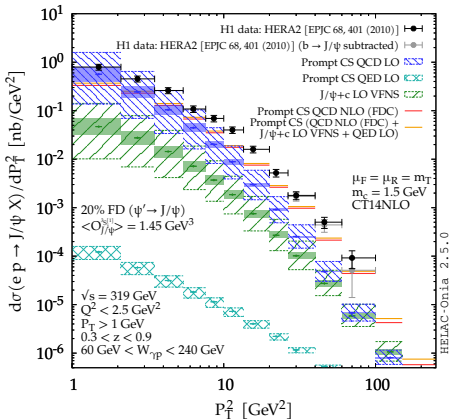


$$\left\{ \begin{array}{l} \gamma + c \rightarrow \psi + c @ \alpha \alpha_s^2 \text{w. 4 Flavour Scheme} \\ \gamma + g \rightarrow \psi + c + \bar{c} @ \alpha \alpha_s^3 \text{w. 3 Flavour Scheme} \end{array} \right. \text{VFNS [also NEW !]}$$

Notes:
 The computations were done with HELAC-ONIA and FDC. The scale and mass uncertainties are shown by the hatched and solid bands.
 HELAC-Onia: H.S. Shao, CPC198 (2016) 238; FDC: J.-X. Wang Nucl.Instrum.Meth. A534(2004)241-245; See also <https://nloaccess.in2p3.fr>

Different contributions in the CSM up to NLO

NLO*: C.Flore, J.-P. Lansberg, H.S. Shao, Y. Yedelkina, PLB 811 (2020) 135926



Notes:

The computations were done with HELAC-ONIA and FDC. The scale and mass uncertainties are shown by the hatched and solid bands.

HELAC-Onia: H.S. Shao, CPC198 (2016) 238; FDC: J.-X. Wang Nucl.Instrum.Meth.

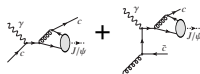
A534(2004)241-245; See also <https://nloaccess.in2p3.fr>



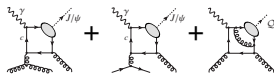
$$\gamma + g \rightarrow \psi + g @ \alpha \alpha_S^2$$



$$\gamma + q \rightarrow \psi + q @ \alpha^3 \text{ [NEW !]}$$



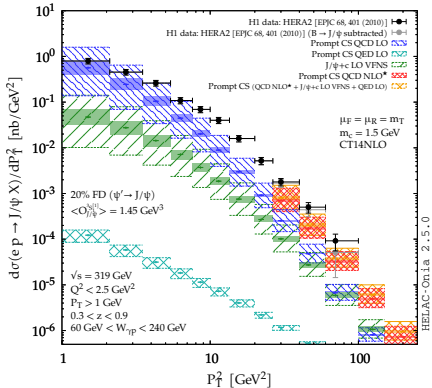
$$\left\{ \begin{array}{l} \gamma + c \rightarrow \psi + c @ \alpha \alpha_S^2 \text{ w. 4 Flavour Scheme} \\ \gamma + g \rightarrow \psi + c + \bar{c} @ \alpha \alpha_S^3 \text{ w. 3 Flavour Scheme} \end{array} \right. \text{VFNS [also NEW !]}$$



$$\left\{ \begin{array}{l} \gamma + g \rightarrow \psi + g + g @ \alpha \alpha_S^3 \\ \gamma + q \rightarrow \psi + g + q @ \alpha \alpha_S^3 \end{array} \right. [+ \gamma g \rightarrow \psi g @ 1L]$$

Different contributions in the CSM up to NLO

NLO*: C.Flore, J.-P. Lansberg, H.S. Shao, Y. Yedelkina, PLB 811 (2020) 135926



$$\gamma + g \rightarrow \psi + g @ \alpha\alpha_s^2$$



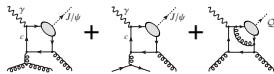
$$\gamma + q \rightarrow \psi + q @ \alpha^3 \text{ [NEW !]}$$



$$\gamma + c \rightarrow \psi + c @ \alpha\alpha_s^2 \text{ w. 4 Flavour Scheme}$$

$$\gamma + g \rightarrow \psi + c + \bar{c} @ \alpha\alpha_s^3 \text{ w. 3 Flavour Scheme}$$

VFNS [also NEW !]



$$\gamma + g \rightarrow \psi + g + g @ \alpha\alpha_s^3$$

$$\gamma + q \rightarrow \psi + g + q @ \alpha\alpha_s^3 \text{ [+ } \gamma g \rightarrow \psi g @ 1L]$$

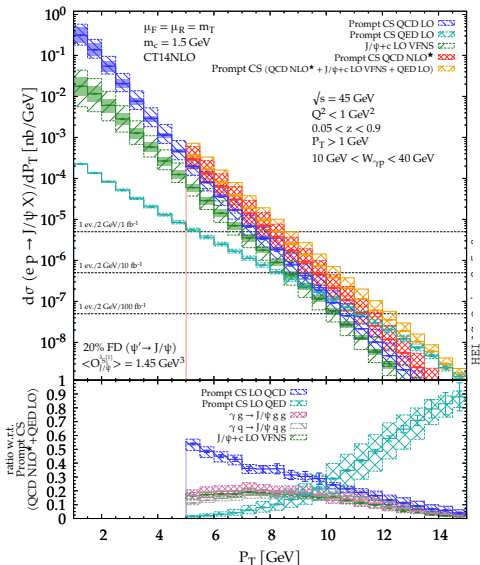
The CSM up to $\alpha\alpha_s^3$ reproduces photoproduction at HERA

Part II

Photoproduction at mid and high P_T at the Electron-Ion Collider

Predictions for the EIC : $J/\psi + X$ ($\sqrt{s_{ep}} = 45$ GeV)

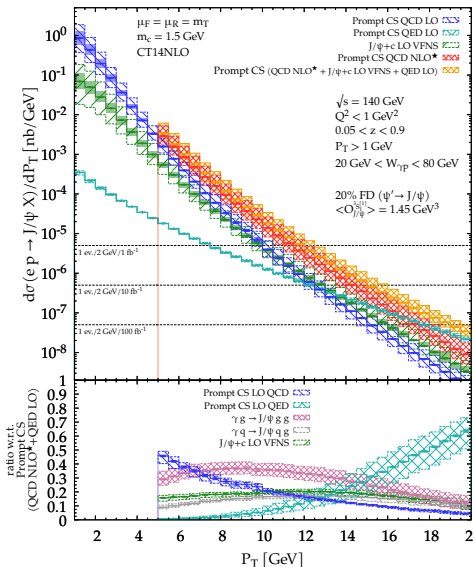
C.Flore, J.-P. Lansberg, H.S. Shao, Y. Yedelkina, PLB 811 (2020) 135926



- At $\sqrt{s_{ep}} = 45$ GeV, one gets into **valence region**
- Yield steeply falling with P_T
- Yield can be measured **up to $P_T \sim 11$ GeV** with $\mathcal{L} = 100$ fb⁻¹
[using both ee and $\mu\mu$ decay channels and $\varepsilon_{J/\psi} \simeq 80\%$]
- QED contribution leading** at the largest reachable P_T
- photon-quark fusion** contributes more than 30 % for $P_T > 8$ GeV

Predictions for the EIC : $J/\psi + X$ ($\sqrt{s_{ep}} = 140$ GeV)

C.Flore, J.-P. Lansberg, H.S. Shao, Y. Yedelkina, PLB 811 (2020) 135926



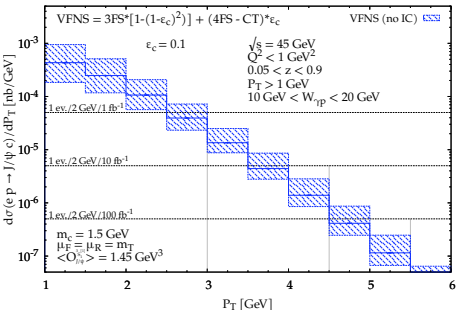
- At $\sqrt{s_{ep}} = 140$ GeV, larger P_T range up to approx. 18 GeV
- QED contribution also leading at the largest reachable P_T
- photon-gluon fusion contributions dominant up to approx. 15 GeV
- $J/\psi + 2$ hard partons [*i.e.* $J/\psi + \{gg, qg, c\bar{c}\}$] dominant for $P_T \sim 8 - 15$ GeV
- It could lead to the observation of $J/\psi + 2$ jets with moderate P_T^{jet}
- with a specific topology where the leading jet_1 recoils on the $J/\psi + \text{jet}_2$ pair
- We expect the $d\sigma$ to vanish when $E_{\text{jet}_2}^{J/\psi \text{ rest fr.}} \rightarrow 0$

Part III

J/ψ +charm associated production at the EIC

J/ψ +charm associated production at the EIC

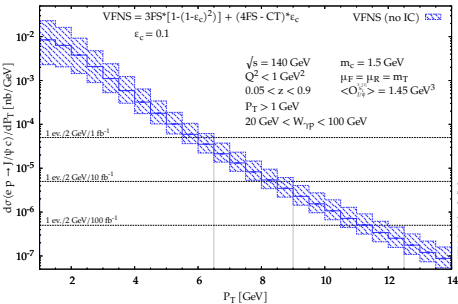
C.Flore, J.-P. Lansberg, H.S. Shao, Y. Yedelkina, PLB 811 (2020) 135926



- Same LO VFNS computation previously shown in green except for the **charm-detection efficiency**
 $\epsilon_C: \sigma^{VFNS} = \sigma^{3FS} \times (1 - (1 - \epsilon)^2) + (\sigma^{4FS} - \sigma^{CT}) \times \epsilon$
- At $\sqrt{s_{ep}} = 45$ GeV, yield limited to **low P_T** even with $\mathcal{L} = 100 \text{ fb}^{-1}$
- But it is clearly observable if $\epsilon_C = 0.1$ with $\mathcal{O}(500, 50, 5)$ **events** for $\mathcal{L} = (100, 10, 1) \text{ fb}^{-1}$

J/ψ + charm associated production at the EIC

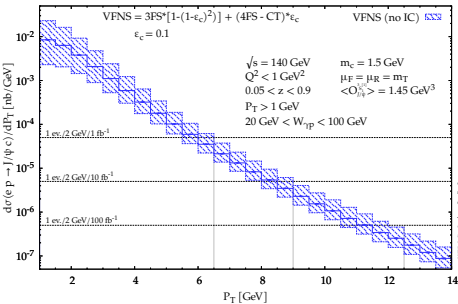
C.Flore, J.-P. Lansberg, H.S. Shao, Y. Yedelkina, PLB 811 (2020) 135926



- Same LO VFNS computation previously shown in green except for the **charm-detection efficiency**
- $$\epsilon_C: \sigma^{VFNS} = \sigma^{3FS} \times (1 - (1 - \epsilon)^2) + (\sigma^{4FS} - \sigma^{CT}) \times \epsilon$$
- At $\sqrt{s_{ep}} = 45$ GeV, yield limited to **low P_T** even with $\mathcal{L} = 100 \text{ fb}^{-1}$
 - But it is clearly observable if $\epsilon_C = 0.1$ with $\mathcal{O}(500, 50, 5)$ **events for $\mathcal{L} = (100, 10, 1) \text{ fb}^{-1}$**
 - At $\sqrt{s_{ep}} = 140$ GeV, P_T range up to 10 GeV with **up to thousands of events with $\mathcal{L} = 100 \text{ fb}^{-1}$**
 - Could be observed via **charm jet**

$J/\psi + \text{charm}$ associated production at the EIC

C.Flore, J.-P. Lansberg, H.S. Shao, Y. Yedelkina, PLB 811 (2020) 135926

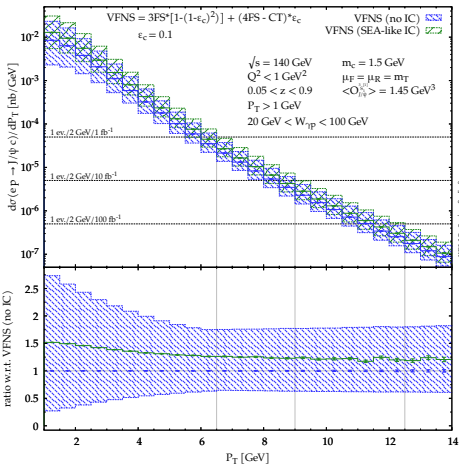


- Same LO VFNS computation previously shown in green except for the **charm-detection efficiency**
- $\epsilon_C: \sigma^{VFNS} = \sigma^{3FS} \times (1 - (1 - \epsilon)^2) + (\sigma^{4FS} - \sigma^{CT}) \times \epsilon$
- At $\sqrt{s_{ep}} = 45 \text{ GeV}$, yield limited to **low P_T** even with $\mathcal{L} = 100 \text{ fb}^{-1}$
- But it is clearly observable if $\epsilon_C = 0.1$ with $\mathcal{O}(500, 50, 5)$ **events for $\mathcal{L} = (100, 10, 1) \text{ fb}^{-1}$**
- At $\sqrt{s_{ep}} = 140 \text{ GeV}$, P_T range up to 10 GeV with **up to thousands of events with $\mathcal{L} = 100 \text{ fb}^{-1}$**
- Could be observed via **charm jet**

- 4FS $\gamma c \rightarrow J/\psi c$ depend on $c(x)$ and could be enhanced by **intrinsic charm**

J/ψ + charm associated production at the EIC

C.Flore, J.-P. Lansberg, H.S. Shao, Y. Yedelkina, PLB 811 (2020) 135926

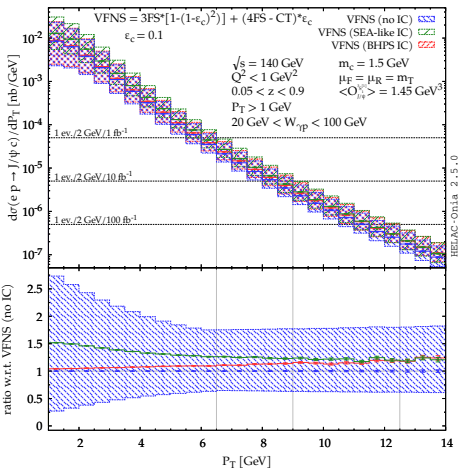


- Same LO VFNS computation previously shown in green except for the **charm-detection efficiency**
 $\epsilon_c: \sigma^{VFNS} = \sigma^{3FS} \times (1 - (1 - \epsilon)^2) + (\sigma^{4FS} - \sigma^{CT}) \times \epsilon$
- At $\sqrt{s_{ep}} = 45 \text{ GeV}$, yield limited to **low P_T** even with $\mathcal{L} = 100 \text{ fb}^{-1}$
- But it is clearly observable if $\epsilon_c = 0.1$ with $\mathcal{O}(500, 50, 5)$ events for $\mathcal{L} = (100, 10, 1) \text{ fb}^{-1}$
- At $\sqrt{s_{ep}} = 140 \text{ GeV}$, P_T range up to 10 GeV with **up to thousands of events** with $\mathcal{L} = 100 \text{ fb}^{-1}$
- Could be observed via **charm jet**

- 4FS $\gamma c \rightarrow J/\psi c$ depend on $c(x)$ and could be enhanced by **intrinsic charm**
- Small effect at $\sqrt{s_{ep}} = 140 \text{ GeV}$ [We used IC $c(x)$ encoded in CT14NNLO]

J/ψ + charm associated production at the EIC

C.Flore, J.-P. Lansberg, H.S. Shao, Y. Yedelkina, PLB 811 (2020) 135926

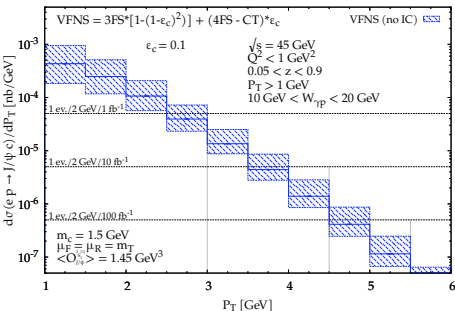


- Same LO VFNS computation previously shown in green except for the **charm-detection efficiency**
- ϵ_c : $\sigma^{VFNS} = \sigma^{3FS} \times (1 - (1 - \epsilon)^2) + (\sigma^{4FS} - \sigma^{CT}) \times \epsilon$
- At $\sqrt{s_{sep}} = 45$ GeV, yield limited to **low P_T** even with $\mathcal{L} = 100 \text{ fb}^{-1}$
- But it is clearly observable if $\epsilon_c = 0.1$ with $\mathcal{O}(500, 50, 5)$ events for $\mathcal{L} = (100, 10, 1) \text{ fb}^{-1}$
- At $\sqrt{s_{sep}} = 140$ GeV, P_T range up to 10 GeV with **up to thousands of events** with $\mathcal{L} = 100 \text{ fb}^{-1}$
- Could be observed via **charm jet**

- 4FS $\gamma c \rightarrow J/\psi c$ depend on $c(x)$ and could be enhanced by **intrinsic charm**
- Small effect at $\sqrt{s_{sep}} = 140$ GeV [We used IC $c(x)$ encoded in CT14NNLO]

J/ψ + charm associated production at the EIC

C.Flore, J.-P. Lansberg, H.S. Shao, Y. Yedelkina, PLB 811 (2020) 135926

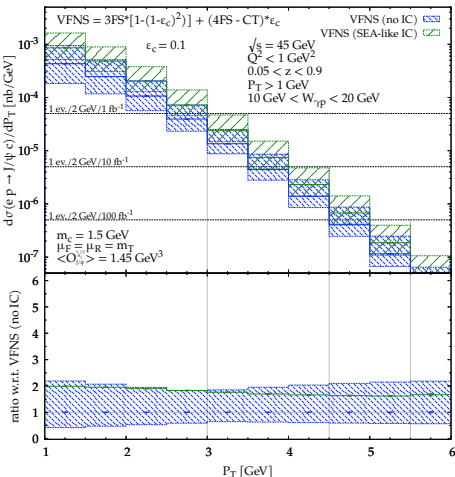


- Same LO VFNS computation previously shown in green except for the **charm-detection efficiency**
 $\epsilon_c: \sigma^{VFNS} = \sigma^{3FS} \times (1 - (1 - \epsilon)^2) + (\sigma^{4FS} - \sigma^{CT}) \times \epsilon$
- At $\sqrt{s_{ep}} = 45$ GeV, yield limited to **low P_T** even with $\mathcal{L} = 100 \text{ fb}^{-1}$
- But it is clearly observable if $\epsilon_c = 0.1$ with $\mathcal{O}(500, 50, 5)$ **events for $\mathcal{L} = (100, 10, 1) \text{ fb}^{-1}$**
- At $\sqrt{s_{ep}} = 140$ GeV, P_T range up to 10 GeV with **up to thousands of events with $\mathcal{L} = 100 \text{ fb}^{-1}$**
- Could be observed via **charm jet**

- 4FS $\gamma c \rightarrow J/\psi c$ depend on $c(x)$ and could be enhanced by **intrinsic charm**
- Small effect at $\sqrt{s_{ep}} = 140$ GeV [We used IC $c(x)$ encoded in CT14NNLO]
- Measurable effect at $\sqrt{s_{ep}} = 45$ GeV

J/ψ + charm associated production at the EIC

C.Flore, J.-P. Lansberg, H.S. Shao, Y. Yedelkina, PLB 811 (2020) 135926

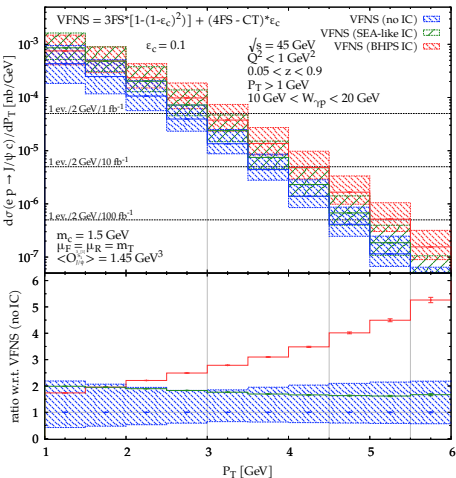


- Same LO VFNS computation previously shown in green except for the **charm-detection efficiency**
 $\epsilon_c: \sigma^{\text{VFNS}} = \sigma^{3\text{FS}} \times (1 - (1 - \epsilon)^2) + (\sigma^{4\text{FS}} - \sigma^{\text{CT}}) \times \epsilon$
- At $\sqrt{s_{ep}} = 45 \text{ GeV}$, yield limited to **low P_T** even with $\mathcal{L} = 100 \text{ fb}^{-1}$
- But it is clearly observable if $\epsilon_c = 0.1$ with $\mathcal{O}(500, 50, 5)$ events for $\mathcal{L} = (100, 10, 1) \text{ fb}^{-1}$
- At $\sqrt{s_{ep}} = 140 \text{ GeV}$, P_T range up to 10 GeV with **up to thousands of events** with $\mathcal{L} = 100 \text{ fb}^{-1}$
- Could be observed via **charm jet**

- 4FS $\gamma c \rightarrow J/\psi c$ depend on $c(x)$ and could be enhanced by **intrinsic charm**
- Small effect at $\sqrt{s_{ep}} = 140 \text{ GeV}$ [We used IC $c(x)$ encoded in CT14NNLO]
- Measurable effect at $\sqrt{s_{ep}} = 45 \text{ GeV}$

J/ψ + charm associated production at the EIC

C.Flore, J.-P. Lansberg, H.S. Shao, Y. Yedelkina, PLB 811 (2020) 135926



- Same LO VFNS computation previously shown in green except for the **charm-detection efficiency**
 $\epsilon_c: \sigma^{VFNS} = \sigma^{3FS} \times (1 - (1 - \epsilon)^2) + (\sigma^{4FS} - \sigma^{CT}) \times \epsilon$
- At $\sqrt{s_{ep}} = 45 \text{ GeV}$, yield limited to **low P_T** even with $\mathcal{L} = 100 \text{ fb}^{-1}$
- But it is clearly observable if $\epsilon_c = 0.1$ with $\mathcal{O}(500, 50, 5)$ events for $\mathcal{L} = (100, 10, 1) \text{ fb}^{-1}$
- At $\sqrt{s_{ep}} = 140 \text{ GeV}$, P_T range up to 10 GeV with **up to thousands of events** with $\mathcal{L} = 100 \text{ fb}^{-1}$
- Could be observed via **charm jet**

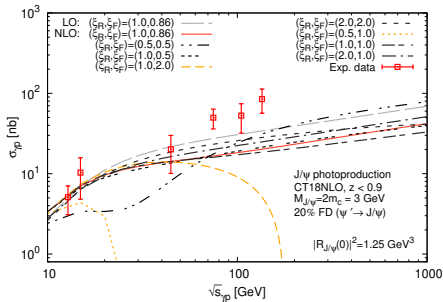
- 4FS $\gamma c \rightarrow J/\psi c$ depend on $c(x)$ and could be enhanced by **intrinsic charm**
- Small effect at $\sqrt{s_{ep}} = 140 \text{ GeV}$ [We used IC $c(x)$ encoded in CT14NNLO]
- Measurable effect at $\sqrt{s_{ep}} = 45 \text{ GeV}$: **BHPS valence-like peak visible!**

Part IV

Study of the impact of the NLO
corrections to P_T -integrated
photoproduction cross section

The negative cross-sections issue at high energies

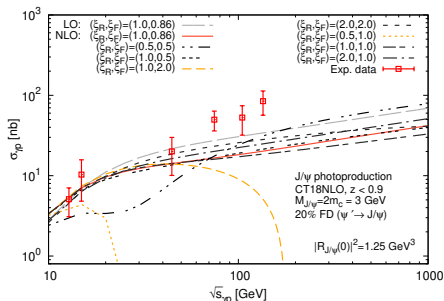
A. Colpani Serri, Y. Feng, C. Flore, J.P. Lansberg, M.A. Ozelik, H.S. Shao, Y. Yedelkina: arXiv:2112.05060 [hep-ph]



Exp. data: H1 - M.Kraemer: NPB 459(1996)3-50, FTPS - B.H.Denby et al.: PRL 52(1984)795-798, NAI - NA14 Collaboration, R.Barate et al.: Z.Phys.C 33(1987)505

The negative cross-sections issue at high energies

A. Colpani Serri, Y. Feng, C. Flore, J.P. Lansberg, M.A. Ozelik, H.S. Shao, Y. Yedelkina: arXiv:2112.05060 [hep-ph]

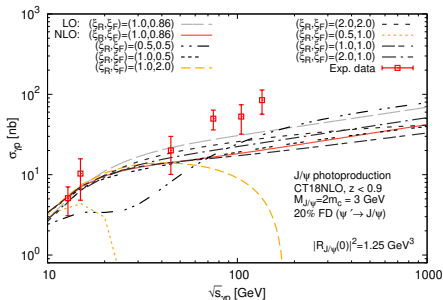


- **NLO** cross section for J/ψ photoproduction becomes negative for **large** μ_F when $\sqrt{s_{\gamma p}}$ increases

Exp. data: H1 - M.Kraemer: NPB 459(1996)3-50, FTPS - B.H.Denby et al.: PRL 52(1984)795-798, NAI - NA14 Collaboration, R.Barate et al.: Z.Phys.C 33(1987)505

The negative cross-sections issue at high energies

A. Colpani Serri, Y. Feng, C. Flore, J.P. Lansberg, M.A. Ozelcik, H.S. Shao, Y. Yedekina: arXiv:2112.05060 [hep-ph]



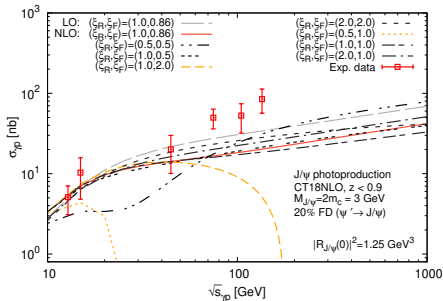
- **NLO** cross section for J/ψ photoproduction becomes negative for **large** μ_F when $\sqrt{s_{\gamma p}}$ increases
- For $\mu_F = 2M$, $\sigma < 0$ as in case of η_c hadroproduction

J.P. Lansberg, M.A. Ozelcik: Eur.Phys.J.C 81 (2021) 6, 497

Exp. data: H1 - M.Kraemer: NPB 459(1996)3-50, FTPS - B.H.Denby et al.: PRL 52(1984)795-798, NAI - NA14Collaboration, R.Barate et al.:Z.Phys.C 33(1987)505

The negative cross-sections issue at high energies

A. Colpani Serri, Y. Feng, C. Flore, J.P. Lansberg, M.A. Ozelik, H.S. Shao, Y. Yedelkina: arXiv:2112.05060 [hep-ph]



- **NLO** cross section for J/ψ photoproduction becomes negative for **large** μ_F when $\sqrt{s_{\gamma p}}$ increases
- For $\mu_F = 2M$, $\sigma < 0$ as in case of η_c hadroproduction

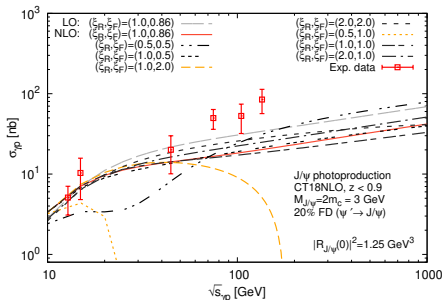
J.P. Lansberg, M.A. Ozelik: Eur.Phys.J.C 81 (2021) 6, 497

- 2 possible sources of negative partonic cross sections: loop corrections (interference) and from real emission (subtraction of IR poles)

Exp. data: H1 - M.Kraemer: NPB 459(1996)3-50, FTPS - B.H.Denby et al.: PRL 52(1984)795-798, NAI - NA14Collaboration, R.Barate et al.:Z.Phys.C 33(1987)505

Negative cross-section values

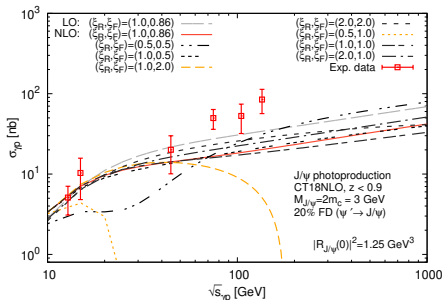
A. Colpani Serri, Y. Feng, C. Flore, J.P. Lansberg, M.A. Ozcelik, H.S. Shao, Y. Yedelkina: arXiv:2112.05060 [hep-ph]



- Initial state collinear divergences are removed via the **subtraction** into the PDFs via AP-CT

Negative cross-section values

A. Colpani Serri, Y. Feng, C. Flore, J.P. Lansberg, M.A. Ozelik, H.S. Shao, Y. Yedelkina: arXiv:2112.05060 [hep-ph]



- Initial state collinear divergences are removed via the **subtraction** into the PDFs via AP-CT

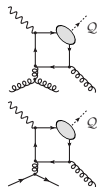
- $\hat{S} \rightarrow \infty : \hat{\sigma}_{\gamma i}^{NLO} \propto \alpha_s(\mu_R) \left(\bar{c}_1^{(\gamma i)} \log \frac{M_Q^2}{\mu_F^2} + c_1^{(\gamma i)} \right), A_{\gamma i} = \frac{c_1^{(\gamma i)}}{\bar{c}_1^{(\gamma i)}}$

$$A_{\gamma g} = A_{\gamma q}$$

A scale prescription for μ_F

J.P. Lansberg, M.A. Ozelik: Eur.Phys.J.C 81 (2021) 6, 497

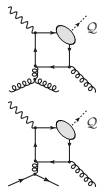
- In principle, such negative terms should be compensated by the **evolution** of the PDFs governed by the DGLAP equations;



A scale prescription for μ_F

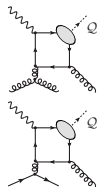
J.P. Lansberg, M.A. Ozelik: Eur.Phys.J.C 81 (2021) 6, 497

- In principle, such negative terms should be compensated by the **evolution** of the PDFs governed by the DGLAP equations;
- $A_{\gamma g}, A_{\gamma q}$ are **process-dependent**, while the DGLAP equations are **process-independent**, which makes the compensation imperfect;



A scale prescription for μ_F

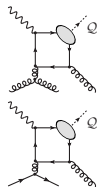
J.P. Lansberg, M.A. Ozelik: Eur.Phys.J.C 81 (2021) 6, 497



- In principle, such negative terms should be compensated by the **evolution** of the PDFs governed by the DGLAP equations;
- $A_{\gamma g}, A_{\gamma q}$ are **process-dependent**, while the DGLAP equations are **process-independent**, which makes the compensation imperfect;
- But as $A_{\gamma g} = A_{\gamma q}$, we can **choose** μ_F such that $\lim_{\hat{s} \rightarrow \infty} \hat{\sigma}_{\gamma i}^{NLO} = 0$

A scale prescription for μ_F

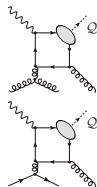
J.P. Lansberg, M.A. Ozelik: Eur.Phys.J.C 81 (2021) 6, 497



- In principle, such negative terms should be compensated by the **evolution** of the PDFs governed by the DGLAP equations;
- $A_{\gamma g}, A_{\gamma q}$ are **process-dependent**, while the DGLAP equations are **process-independent**, which makes the compensation imperfect;
- But as $A_{\gamma g} = A_{\gamma q}$, we can **choose** μ_F such that $\lim_{\hat{s} \rightarrow \infty} \hat{\sigma}_{\gamma i}^{NLO} = 0$
- This amounts to consider that all the QCD corrections are in the PDFs

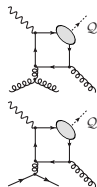
A scale prescription for μ_F

J.P. Lansberg, M.A. Ozelik: Eur.Phys.J.C 81 (2021) 6, 497



- In principle, such negative terms should be compensated by the **evolution** of the PDFs governed by the DGLAP equations;
- $A_{\gamma g}, A_{\gamma q}$ are **process-dependent**, while the DGLAP equations are **process-independent**, which makes the compensation imperfect;
- But as $A_{\gamma g} = A_{\gamma q}$, we can **choose** μ_F such that $\lim_{\hat{s} \rightarrow \infty} \hat{\sigma}_{\gamma i}^{NLO} = 0$
- This amounts to consider that all the QCD corrections are in the PDFs
- The choice of factorisation scale to avoid possible negative hadronic cross-section: (for $\eta_Q : A_{gi} = -1$)
 $\mu_F = \hat{\mu}_F = M e^{A_{\gamma i}/2};$

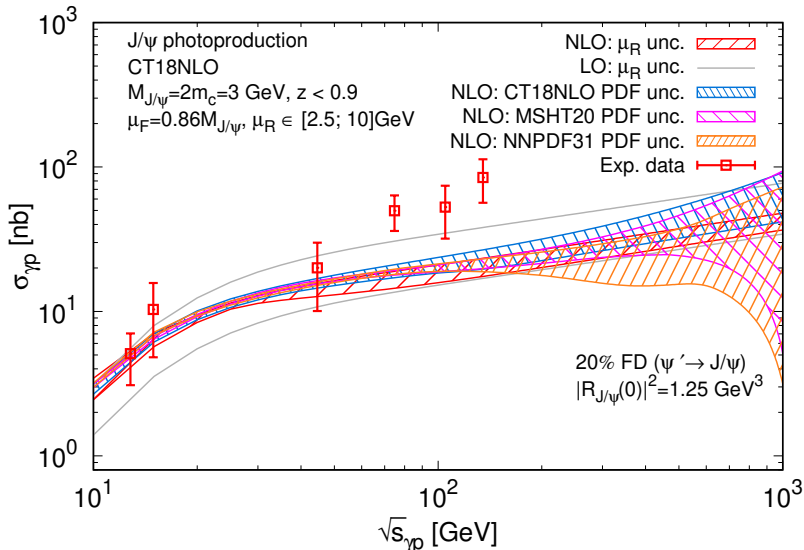
A scale prescription for μ_F



- In principle, such negative terms should be compensated by the **evolution** of the PDFs governed by the DGLAP equations;
- $A_{\gamma g}, A_{\gamma q}$ are **process-dependent**, while the DGLAP equations are **process-independent**, which makes the compensation imperfect;
- But as $A_{\gamma g} = A_{\gamma q}$, we can **choose** μ_F such that $\lim_{\hat{s} \rightarrow \infty} \hat{\sigma}_{\gamma i}^{NLO} = 0$
- This amounts to consider that all the QCD corrections are in the PDFs
- The choice of factorisation scale to avoid possible negative hadronic cross-section: (for $\eta_Q : A_{gi} = -1$)
 $\mu_F = \hat{\mu}_F = M e^{A_{\gamma i}/2};$
- For J/ψ (Y) photoproduction: $\hat{\mu}_F = 0.86M$
($P_T \in [0, \infty], z < 0.9$)

Results with $\hat{\mu}_F = 0.85M$

A. Colpani Serri, Y. Feng, C. Flore, J.P. Lansberg, M.A. Ozcelik, H.S. Shao, Y. Yedelkina: arXiv:2112.05060 [hep-ph]



Exp. data: H1 - M.Kraemer: Nucl.Phys.B 459(1996)3-50, FTPS - B.H.Denbyet al.: Phys.Rev.Lett. 52(1984)795-798, NAI - NA14Collaboration, R.Barateet al.: Z.Phys.C 33(1987)505

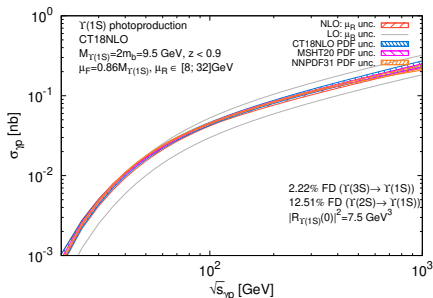
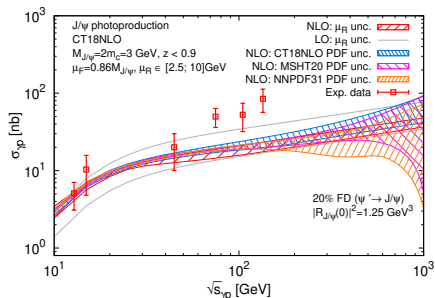
Part V

Can J/ψ & Υ allow us to probe PDFs? :
PDF vs scale uncertainties

J/ ψ & Υ : PDF uncertainties of $\sigma(\sqrt{s_{\gamma p}})$

A. Colpani Serri, Y. Feng, C. Flore, J.P. Lansberg, M.A. Ozelcik, H.S. Shao, Y. Yedelkina: arXiv:2112.05060 [hep-ph]

- PDF uncertainties increase at large \sqrt{s} (i.e. small x)
- The μ_R unc. are reduced at NLO in comparison with LO

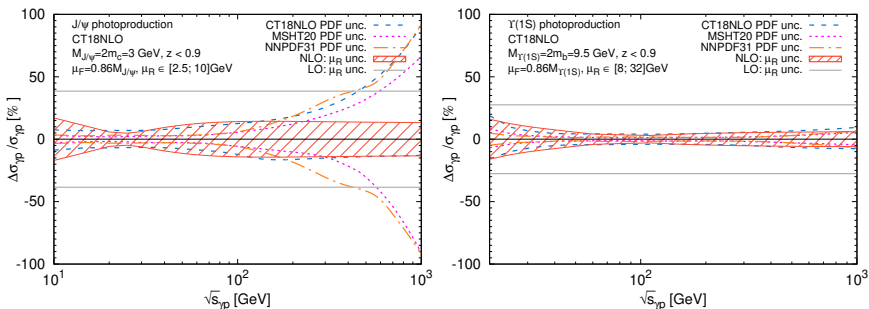


Exp. data: H1 - Nucl.Phys.B 472(1996)3-31, FTPS - B.H.Denby et al.: PRL 52(1984)795-798, NAI - NA14Collaboration, R.Barate et al.:Z.Phys.C 33(1987)505

J/ψ & Υ : PDF uncertainties of $\sigma(\sqrt{s_{\gamma p}})$

A. Colpani Serri, Y. Feng, C. Flore, J.P. Lansberg, M.A. Ozcelik, H.S. Shao, Y. Yedelkina: arXiv:2112.05060 [hep-ph]

- PDF uncertainties increase at large \sqrt{s} (i.e. small x)
- The μ_R unc. are reduced at NLO in comparison with LO
- Increase of μ_R unc. from $\sqrt{s_{\gamma p}} \gtrsim 50$ GeV from the loop corr.
- At NNLO we expect a further reduction of μ_R uncertainties



Exp. data: H1 - Nucl.Phys.B 472(1996)3-31, FTPS - B.H.Denby et al.: PRL 52(1984)795-798, NAI - NA14Collaboration, R.Barate et al.:Z.Phys.C 33(1987)505

Exp.	$\sqrt{s_{ep}}$	\mathcal{L} (fb $^{-1}$)	$N_{J/\psi}$	$N_{Y(1S)}$
EicC	16.7	100	$1.5^{+0.3}_{-0.2} \cdot 10^6$	$2.3^{+1.1}_{-1.4} \cdot 10^0$
AMBER	17.3	1	$1.6^{+0.3}_{-0.3} \cdot 10^4$	< 1
EIC	45	100	$8.5^{+0.5}_{-1.0} \cdot 10^6$	$6.1^{+0.7}_{-0.8} \cdot 10^2$
EIC	140	100	$2.5^{+0.1}_{-0.4} \cdot 10^7$	$7.6^{+0.3}_{-0.7} \cdot 10^3$
LheC	1183	100	$9.3^{+2.9}_{-2.9} \cdot 10^7$	$8.1^{+0.4}_{-0.7} \cdot 10^4$
FCC-eh	3464	100	$1.6^{+0.2}_{-1.0} \cdot 10^8$	$1.8^{+0.1}_{-0.2} \cdot 10^5$

We expect μ_R unc. to shrink at NNLO:

Possibility to constrain PDF with differential measurements

Rem. $N_{\psi'} \simeq 0.08 \times N_{J/\psi}$, $N_{Y(2S)} \simeq 0.4 \times N_{Y(1S)}$, $N_{Y(3S)} \simeq 0.35 \times N_{Y(1S)}$

Part VI

Conclusions

Conclusions

- The CSM up to $\alpha\alpha_s^3$ reproduces photoproduction at HERA up to scale-uncertainty
- The estimations for EIC can rely on CSM only

Conclusions

- The CSM up to $\alpha\alpha_s^3$ reproduces photoproduction at HERA up to scale-uncertainty
- The estimations for EIC can rely on CSM only
- NLO QCD corrections are important for P_T -integrated σ
- A specific μ_F choice can be employed to avoid a possible over subtraction of collinear divergences which lead to negative NLO σ values at large $\sqrt{s_{\gamma p}}$
- Loop correction matter and significant NNLO corrections (likely positive) are expected as well as a further reduction of the μ_R unc., esp. around 100 GeV
- This would likely allow one to better probe gluon PDFs at small- x and $\mu_F \sim M$.

Backup

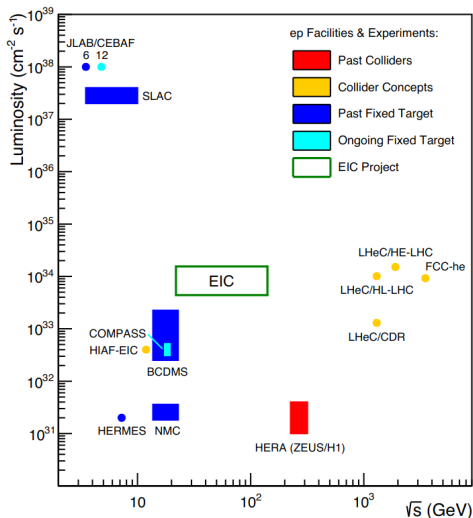
Resolved-photon contributions

J.P. Lansberg, Phys.Rept. 889 (2020)

- At high energies, the hadronic content of the photon can be 'resolved' during the collisions
- Are very similar to those for hadroproduction
- At low z they can appear as important where only a small fraction of the photon energy is involved in the quarkonium production (limited impact at HERA)
- At lower energies, like at the EIC, their impact should be further reduced
- Can be avoided by a simple kinematical cut on low elasticity values, z
- It will be needed to re-evaluate its impact

The Electron Ion Collider at BNL

Abhay Deshpande EIC @ BNL, HiX at Kolympari



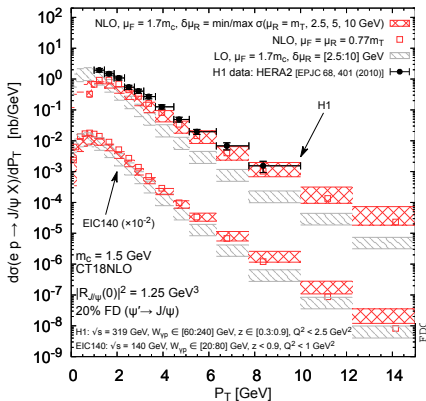
- Hadrons up to 275 GeV
- Electrons up to 5-10(20) GeV
- CoM \sqrt{s} : 20-100 (140) GeV
- High luminosity
 $L_{ep} \propto 10^{33-34} \text{ cm}^{-2} \text{ sec}^{-1}$
 (100-1000 times HERA)
- World's first:
 - ▶ collider with polarized (min 70%) lepton & proton/light-ion beams
 - ▶ electron-Nucleus collider

Feed down

C.Flore, J.-P. Lansberg, H.S. Shao, Y. Yedelkina, PLB 811 (2020) 135926

- **b FD** (5% on the P_T -integrated yields and is significant around $P_T = 10$ GeV): we do not include it as it can be experimentally removed.
- Tune Pythia 8.2 using a b analysis by H1 using di-electrons events which extends to large P_T
 - ▶ Compute the corresponding LO+PS cross section using Pythia 8.2
 - ▶ Perform a χ^2 -minimisation to compute a tuning factor (absorbs the theory uncertainties), such that the obtained LO+PS Pythia spectrum reproduces best the H1 b data
 - ▶ Again use Pythia 8.2 to compute the $b \rightarrow J/\psi$ cross section in the H1 kinematics.
 - ▶ Subtract this $b \rightarrow J/\psi$ yield from the inclusive one
- χ_c FD: no theory or experimental indication that it could be relevant
- 20% ψ' FD: follows from the ratio of the wave functions at the origin and from the $\psi' \rightarrow J/\psi$ branching: $FD_{\psi' \rightarrow J/\psi} = |R_{\psi'}(0)|^2 / |R_{J/\psi}(0)|^2 Br(\psi' \rightarrow J/\psi)$

P_T -differential cross sections



- If p_T -dependence is taken into account, for $\hat{s} \rightarrow \infty$:

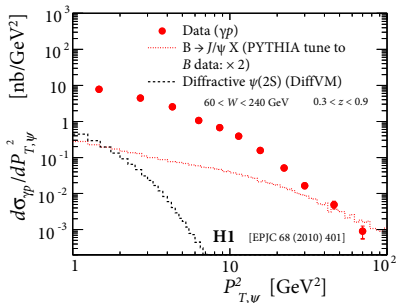
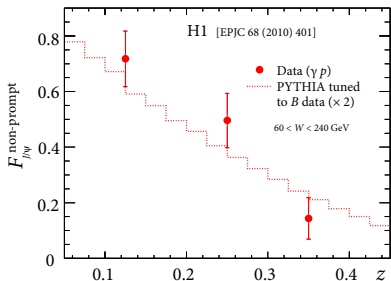
$$c_1^{(\gamma i)}(p_T) / \bar{c}_1^{(\gamma i)}(p_T) \propto (P_T / M_Q)^2$$
- $\Rightarrow \hat{\mu}_F = M e^{c_{\gamma i}^{(1)} / 2\bar{c}_{\gamma i}^{(1)}} \propto M e^{P_T^2 / M^2}$,
 which is weird
- Full matched calculation between NLO and $\ln \hat{s} / M^2$ -resummation is needed
- Common dynamical scale choice:

$$\mu_F = (0.5, 1, 2) m_T$$

- one can use $\mu_F = \alpha \sqrt{M^2 + P_T^2}$ or $\mu_F = \sqrt{(\beta M)^2 + P_T^2}$
- if P_T is large, then $\mu_F \propto P_T$
- For $\mu_F = \hat{\mu}_F$ with $\langle P_T^2 \rangle = 2.5 \text{ GeV}^2$ (for J/ψ at HERA energies), we get $\alpha = 0.77$ and $\beta = 0.7$

Feed down

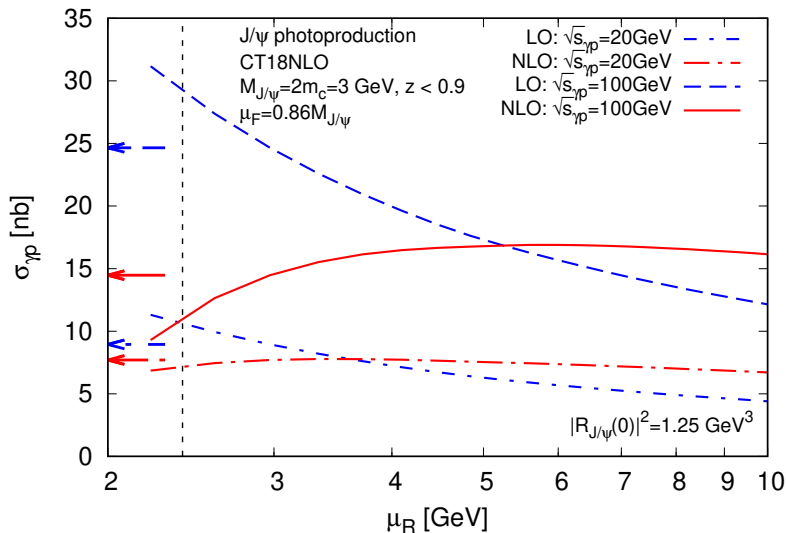
J.P. Lansberg, Phys.Rept. 889 (2020); C.Flore, J.-P. Lansberg, H.S. Shao, Y. Yedelkina, PLB 811 (2020) 135926



- **b FD** (5% on the P_T -integrated yields and can go up to $\approx 50\%$ at $P_T = 10$ GeV): we do not include it as it can be experimentally removed.
- χ_c FD: no theory or experimental indication that it could be relevant
- 20% ψ' FD: follows from the ratio of the wave functions at the origin and from the $\psi' \rightarrow J/\psi$ branching:

$$FD_{\psi' \rightarrow J/\psi} = |R_{\psi'}(0)|^2 / |R_{J/\psi}(0)|^2 Br(\psi' \rightarrow J/\psi)$$

Dependence of $\sigma_{\gamma p}$ on the μ_R at an initial photon energy $s_{\gamma p}$



$\hat{\mu}_F$ -prescription as $\ln 1/\hat{z}$ resummation

J.P. Lansberg, M.Nefedov, M.A. Ozcelik: 2112.06789 [hep-ph];

- Mellin transform: $f(N) = \int_0^1 dx x^{N-1} f(x)$ maps $\ln 1/x$ to the $1/N$ poles: $\alpha_s^n \ln^{n-1} \frac{1}{\hat{z}} \rightarrow \frac{\alpha_s^n}{N^n}$, where $\hat{z} = \frac{M^2}{\hat{s}}$
- LO DGLAP splitting at $z \rightarrow 0$:

$$\frac{\alpha_s}{2\pi} z P_{gg}(z) \simeq \frac{\alpha_s C_A}{\pi} \rightarrow \gamma_{gg}(N) \simeq \frac{\alpha_s C_A}{\pi N}$$

\Rightarrow solution of DGLAP equation in N -space

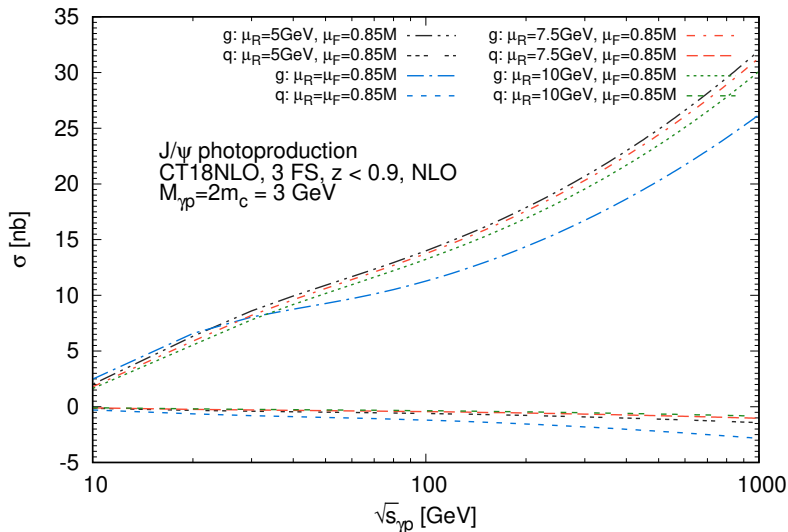
($\frac{\partial f_g(N, \mu_F)}{\partial \ln \mu_F^2} = \gamma_{gg}(N) f_g(N, \mu_F^2)$) in the DLA ($[\alpha_s/N \ln \mu_F]^n$) with

$\hat{\mu}_F = \mu_0 e^{A/2}$ is:

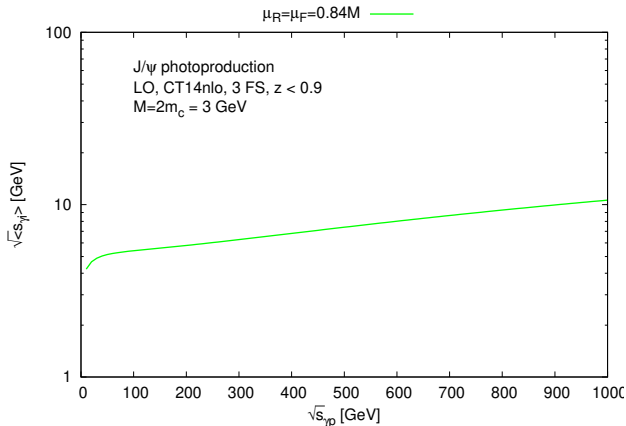
$$f(N, \hat{\mu}_F) \approx f(N, \mu_0) \exp\left(\frac{2A\alpha_s(\mu_0)C_A}{\pi N}\right),$$

\Rightarrow In the exponent we did some approximate resummation of collinear emission contributions for $\hat{s} \rightarrow \infty$.

q& g contributions



μ_R choice



- 1 the natural scale choice in case of J/ψ photoproduction is not a mass of c -quark, because of some loop corrections.
- 2 For J/ψ :
 $\mu_{Rmin} = 1.6m_c$
($\sqrt{s_{\gamma p}} = 10\text{GeV}$)